BMC Complementary Medicine and Therapies

RESEARCH

Open Access

Based on network pharmacology and molecular docking technology to explore the pharmacodynamic components and mechanism of *Gynostemmae Pentaphylli Herba* reversing Cervical intraepithelial neoplasia

Huifang Wang[1*†], Yiling Chen[2†] and Tingting Lin[3]

Abstract

Objective To investigate the pharmacodynamic components of *Gynostemmae Pentaphylli Herba* reversing Cervical intraepithelial neoplasia (CIN) were investigated by network pharmacology, and the mechanism of action was analyzed by molecular docking technology.

Methods The effective components and targets of *Gynostemmae Pentaphylli Herba* and the disease target of CIN were searched in TCMSP, Pubchem, Swiss Target Prediction, GenCards, WebGestalt, and STRING. Based on the above data and the Cytoscape software, we mapped the protein–protein interaction (PPI) co-expression network. The mechanism of *Gynostemmae Pentaphylli Herba* CIN treatment was identified from the enrichment analysis perspective. We performed molecular docking on the AutoDock. Finally, we carried out cell experiments for verification.

Results Eighty-five targets matching the active ingredients of *Gynostemmae Pentaphylli Herba*, and 2512 CIN-related action targets were obtained. The nodal degree values of five components and the target of *Gynostemmae Pentaphylli Herba* in the top 5 were IL6, IL1β, TNF, TP53, and PTGS2. There were 52 intersection targets of the effective active ingredient of *Gynostemmae Pentaphylli Herba* and CIN. The PPI network map suggested that the main active ingredient MOL000098 (Quercetin) had the most targets (40), followed by MOL000351 (Rhamnazin) (17). Gene Ontology (GO) analysis yielded the regulation of transcription from RNA polymerase II promoter, cytoplasm, extracellular space and enzyme binding, zinc ion binding, etc. The Kyoto Encyclopedia of Genes and Genomes (KEGG) pathway identified 114 signaling pathways. These pathways were mainly enriched in positive regulation of transcription from RNA polymerase II promoter, positive regulation of gene expression, cytoplasm, extracellular space, enzyme binding, zinc ion binding, Pathways in cancer, Fluid shear stress and atherosclerosis, etc. The binding energies of IL6, IL1β, TNF, TP53, and PTGS2 with Quercetin, Rhamnazin, Gypenoside XXVII_qt and Gypenoside XXVIII_qt were all

†Huifang Wang and Yiling Chen are co first authors.

*Correspondence:
Huifang Wang
wanghuifang1313@163.com
Full list of author information is available at the end of the article

less than -5 kcal·mol^{-1}, respectively. The messenger ribonucleic acid (mRNA) expressions of IL6, IL1β, TNF, and PTGS2 in the experimental group were higher (t = 105.700, 32.450, 18.190, and 100.400, all $P < 0.001$), and the mRNA expressions of TP53 was lower compared with the control group (t = 8.362, all $P = 0.001$).

Conclusion *Gynostemmae Pentaphylli Herba* may reverse CIN through targeted action of Quercetin, Rhamnazin, and gypenosides, as well as various pathways. Our study preliminarily explored the pharmacodynamic components and mechanism of the reversal of CIN by *Gynostemmae Pentaphylli Herba* and verified the possible mechanism of action through cell and molecular biology experiments to understand the pharmacological mechanism of *Gynostemmae Pentaphylli Herba* in CIN and provide data reference for new drugs and clinical trials research, which will be of great significance for clinical treatment decisions.

Keywords Network pharmacology, Molecular docking, *Gynostemmae Pentaphylli Herba*, Cervical intraepithelial neoplasia, Pharmacodynamic components, Mechanism

Introduction

Cervical cancer ranks second among female malignancies, with persistently high incidence and mortality rates. Moreover, there is an increasingly obvious trend of younger-onset cases, posing a serious threat to women's health [1]. The precancerous lesions of cervical cancer develop relatively slowly and exhibit significant gradual characteristics. Generally, it progresses from cervical intraepithelial neoplasia (CIN) to carcinoma in situ, and then to invasive carcinoma [2, 3]. As a precancerous lesion of cervical cancer, CIN has a 15%–45% probability of progressing to cervical cancer [4]. Currently, loop electrosurgical excision procedure (LEEP) is the main clinical treatment for CIN. Although this method has advantages such as minimal pain, high surgical safety, and good efficacy, it still has certain impacts on patients' post-operative pregnancy [5].

In the field of cancer prevention and treatment, traditional Chinese medicine (TCM) has always received extensive attention. Numerous studies have demonstrated the potential application value of various Chinese herbal medicines and their extracts in cancer treatment. However, among the many Chinese herbal medicines with anti-cancer potential, our choice to conduct in-depth research on *Gynostemmae Pentaphylli Herba* is based on multiple considerations. On one hand, relevant studies have shown that aptamer-modified *Gynostemmae Pentaphylli Herba* can counteract tumors [6], and gypenosides can inhibit the growth of cervical cancer HeLa cells [7], suggesting that *Gynostemmae Pentaphylli Herba* may have unique effects in the treatment of cervical cancer. On the other hand, as a common Chinese herbal medicine, *Gynostemmae Pentaphylli Herba* has been widely used in traditional medicine, with relatively rich application experience and a safety basis. Compared with some other Chinese herbal medicines with similar anti-cancer potential, although research on *Gynostemmae Pentaphylli Herba* is not yet in-depth, the existing preliminary research results have provided certain clues and a basis for its application in the treatment of cervical precancerous lesions. At the same time, the relatively abundant resources of *Gynostemmae Pentaphylli Herba* provide a good material basis for subsequent research and possible clinical applications. Nevertheless, the specific effects of *Gynostemmae Pentaphylli Herba* on cervical cancer are still unclear, especially the mechanism of its treatment of CIN, which has been less studied in the medical community. Clearly understanding the mechanism of action of *Gynostemmae Pentaphylli Herba* in cancer is of great significance for guiding clinical treatment decisions and developing new anti-cancer drugs.

In recent years, network pharmacology and molecular docking techniques have achieved fruitful results in TCM research, providing new ideas for exploring the pharmacodynamic components and mechanisms of action of TCM. For example, the research published by Ma et al. [8] in Phytomedicine, through the combined use of network pharmacology and multi-omics analysis, revealed the key role of the leukotriene pathway in leukopenia and confirmed that ALOX5 is the active target of Qijiao Shengbai Capsule in the treatment of this condition. Another study on the treatment of cerebrovascular diseases with Daqinjiao Decoction [9] utilized network pharmacology to screen for active components and potential targets, combined with molecular docking to verify the binding ability, and through animal model experiments, found that it can act on key targets such as caspase3 and p53, and regulate signaling pathways such as tumor, IL-17, and TNF to exert therapeutic effects.

To understand the pharmacological mechanism of *Gynostemmae Pentaphylli Herba* in CIN, we applied network pharmacology methods and molecular docking techniques to explore the pharmacodynamic components and mechanisms of *Gynostemmae Pentaphylli Herba* in reversing CIN, and verified the possible mechanisms of action through cell molecular biology experiments, aiming to provide data references for new drug development and clinical trials.

Materials and methods

Acquisition of active ingredients and potential drug targets of gynostemma pentaphyllum

The TCMSP database [10] (https://old.tcmsp-e.com/tcmsp.php) was selected as the primary source for screening the active ingredients of gynostemma pentaphyllum. This is because this database integrates extensive pharmacokinetic information of traditional Chinese medicine components, providing a comprehensive and reliable data foundation for the study. The screening criteria were set as an oral bioavailability (OB) of over 30% and a drug likeness (DL) of over 0.18 [11]. The reason for choosing OB > 30% as the screening threshold is that oral bioavailability is a crucial indicator for measuring the absorption of a drug into the systemic circulation after oral administration. A higher oral bioavailability implies that the drug can be more effectively absorbed and utilized by the body, thereby exerting its pharmacological effects. Studies have shown that the oral bioavailability of many clinically effective drugs is usually above 30%. Therefore, using this value as a boundary helps to screen out components that may have actual efficacy in the body. As for setting DL > 0.18, drug likeness is used to evaluate the similarity of a compound to known drugs in terms of structure and properties. A DL value greater than 0.18 generally indicates that the compound possesses physicochemical properties and pharmacokinetic characteristics similar to those of drugs, and preliminarily has the potential to become a drug. This threshold has also been widely applied in relevant research on screening active ingredients of traditional Chinese medicine.

After obtaining all the components of gynostemma pentaphyllum from the TCMSP database, the corresponding targets were screened to obtain the action targets corresponding to the active ingredients of gynostemma pentaphyllum. Subsequently, these targets were standardized using UniProt (https://www.uniprot.org/), with the restricted species specifically set as "human" to ensure that the obtained targets are directly related to human physiological processes and to exclude interference from other species. By eliminating duplicate and non-standard targets, the targets matched with the active ingredients were finally obtained.

During the research process, other similar databases such as PubChem were also considered. The PubChem database contains abundant chemical substance information. However, its focus is on the chemical structure and related properties of compounds, lacking the systematic integration of pharmacokinetic characteristics of traditional Chinese medicine components as in the TCMSP database. Thus, it cannot directly meet the requirements of this study for screening active ingredients based on OB and DL. Therefore, it was not selected as the primary screening database.

Collection of CIN targets

Using "Cervical intraepithelial neoplasia" as the keyword, a search was conducted in the Genecards database (https://www.genecards.org/). The Genecards database integrates a large amount of information on the functions, expressions, and disease associations of human genes, providing comprehensive and authoritative data support for obtaining CIN-related action targets.

Screening of common targets and key targets between gynostemma pentaphyllum and CIN

The Venn diagram was drawn using the Venn diagram-making website (https://bioinfogp.cnb.csic.es/tools/venny/) to obtain the common targets of gynostemma pentaphyllum in the treatment of CIN. This website was chosen because of its simplicity in operation and its ability to visually display the intersection relationships between different datasets.

The obtained common targets were input into STRING version 11.5 (https://www.string-db.org). Specifically, the species was selected as human (Homo sapiens), and data with a confidence level higher than 0.7 were chosen. The confidence level in the STRING database reflects the reliability of the predicted protein–protein interaction (PPI) relationships. Choosing a confidence level > 0.7 is because a higher confidence level implies that the predicted PPI relationships are more likely to exist in biological processes, effectively reducing false-positive results. In the field of protein-interaction research, it is generally recognized that PPI relationships reflected by data with a confidence level higher than 0.7 have a high degree of biological relevance and reliability. Therefore, this was adopted as the screening criterion to ensure that the constructed PPI network diagram can more accurately reflect the real biological processes. Based on these data, a PPI network diagram was constructed. Subsequently, the.tsv data file was imported into the Cytoscape 3.9.1 software for visual mapping.

Based on the cytoHubba plugin, genes were ranked according to the Maximal clique centrality (MCC) score and Degree to determine the key targets. The MCC score can measure the centrality of nodes in the network, while Degree reflects the degree of connection between nodes and other nodes. Through the comprehensive consideration of these two indicators, the targets that may play a key role in the treatment of CIN by gynostemma pentaphyllum can be accurately screened.

GO and KEGG enrichment analysis

Enrichment analysis was carried out based on the WebGestalt database (http://www.webgestalt.org/) [12]. This database provides rich functional annotation and enrichment analysis tools, effectively meeting the needs of this study for gene function and pathway enrichment analysis. After importing the key targets, the Over-Representation (ORA) and BH methods were set for FDR correction. With the corrected false discovery rate (FDR) < 0.05 as the screening criterion, Gene Ontology (GO) [(Biological Process (BP), Molecular Function (MF), and Cellular Component (CC))] and Kyoto Encyclopedia of Genes and Genomes (KEGG) enrichment analyses were performed.

The ORA method was selected because it is widely used in gene-set enrichment analysis and can effectively identify the functional categories significantly enriched in a specific gene set. The BH method is used to control the false discovery rate in multiple hypothesis testing, ensuring the reliability of the analysis results. After performing a weighted analysis of the analysis data, a histogram was drawn to visually display the enrichment levels of different functional categories and pathways.

Small ligand molecules dock with receptor proteins

We completed the docking between ligand small molecules and receptor proteins by the AutoDock software. Finally, PyMOL software visualized the molecular docking model. The binding energy is lower than −5 kal·mol^{-1}, indicating that the protein can bind well with small molecules.

Cell molecular biology experiment

Preparation of Gynostemmae Pentaphylli Herba

Gypenoside (Lot number: B20621-20 mg, Manufacturer: Shanghai Yuanye Bio-Technology Co., Ltd.) was taken and diluted with sterile PBS (Product number: AR0030, Manufacturer: Beijing Solarbio Science & Technology Co., Ltd.) to prepare gynostemma pentaphyllum extracts with concentrations of 0, 100, 300, 400, 500, 600, 700, 800, 900, and 1000 μg/mL, respectively. To avoid batch-to-batch variation, both the Gypenoside and PBS used in the same batch of experiments were from the same production batch. During the experimental process, the consistency of operations was ensured, including the standard use of pipettes during dilution and the degree of uniform mixing.

Cell culture

Cervical cancer HeLa/SiHa cells were purchased from the Shanghai Institute of Cell Biology. RPMI 1640 medium was prepared by adding 10% fetal bovine serum (Lot number: BS-1105, Manufacturer: Shanxi Aopusei Technology Co., Ltd.) and 1% penicillin–streptomycin to DMEM (Dulbecco's Modified Eagle Medium, Product number: c3130-0500, Manufacturer: Shanghai Maxin Biotechnology Co., Ltd.) medium. The cells were cultured in an incubator with 5% carbon dioxide at a temperature of 37 °C, and the medium was changed once a day. To control for batch effects, the same batch of DMEM medium, fetal bovine serum, and penicillin–streptomycin was used throughout all cell culture processes. Moreover, the parameters of the incubator were kept stable, and the medium was replaced daily by dedicated personnel following standardized operating procedures.

CCK8 assay

Cells in the logarithmic growth phase were taken and treated with different concentrations of gynostemma pentaphyllum extracts (0, 100, 300, 400, 500, 600, 700, 800, 900, 1000 μg/mL) respectively, to detect the effects of different concentrations of gynostemma pentaphyllum extracts on the proliferation rate of SiHa cells. Then, curves were plotted to identify the optimal concentration of gynostemma pentaphyllum that inhibits SiHa cells. To minimize batch effects, the same batch of cells, gynostemma pentaphyllum extracts, and CCK-8 reagents was used throughout the entire experiment. The operations of treating cells with different concentrations of gynostemma pentaphyllum extracts were completed within the same time period, and consumables such as cell culture plates and pipettes used were all from the same batch.

Subsequently, cervical cancer HeLa/SiHa cells intervened with the optimal concentration were used as the experimental group, while cervical cancer HeLa/SiHa cells without gynostemma pentaphyllum intervention were used as the control group. Then, the two groups of cells were respectively inoculated into 96-well plates at an inoculation density of 4×10^3 cells/well. On the next day, the medium was removed. Subsequently, 100 μL of alkaline RPIM 1640 medium or basic F12K medium (containing 10 μL of CCK8) was added to the two groups of cells respectively. The cells were incubated for another 2 h, and the optical density was measured at 450 nm using a microplate reader (victor31420 Multilabel Counter, Perkin Elmer, USA). The Cell Counting Kit-8 (CCK-8, Beyotime, China) was used to detect and evaluate cell proliferation, and a CCK8 growth curve was plotted with time gradients of 24, 48, 72, 96, and 120 h. Each time the optical density was measured, it was ensured that the parameter settings of the microplate reader were consistent, and the measurement process was carried out under the same environmental conditions.

Cells were treated with the optimal concentration of gynostemma pentaphyllum extract (the concentration with the lowest OD value and the lowest number

of viable cervical cancer HeLa/SiHa cells) to conduct a colony-forming assay and an EdU proliferation assay to observe the cell proliferation ability, and a scratch assay to observe the cell migration ability.

Clone formation assay

Cervical cancer HeLa/SiHa cells were seeded into 6-well plates at a density of approximately 1000 cells per well and cultured for 14 days. The cells were washed three times with phosphate-buffered saline, fixed in 4% paraformaldehyde (CAS: 30,525–89-4, Wuhan Jiyesheng Chemical Co., LTD) for 30 min, and then stained with 0.5% crystal violet (CAS: G1063, Shanghai Jing Anti biological Engineering Co., LTD). To reduce batch-to-batch variation, the same batch of cells, 6-well plates, phosphate-buffered saline, paraformaldehyde, and crystal violet was used throughout the entire colony-forming assay. During the cell-seeding process, the inoculation density in each well was ensured to be uniform, and the culture environment was kept stable.

EdU (5-Ethynyl-2′-deoxyuridine) assay

The cell invasion assay was conducted in transwell chambers coated with Matrigel (BD biosciences, Bedford, USA). After 48 h of transfection, 1×10^5 cervical cancer HeLa/SiHa cells were seeded into the upper chamber with serum-free medium. Conversely, FBS containing 20% medium was added to the lower chamber. After 48 h of incubation, the invading cells were fixed with 4% paraformaldehyde and stained with 0.5% crystal violet. To avoid batch-to-batch variation, all transwell chambers, Matrigel, cells, serum-free medium, FBS, paraformaldehyde, and crystal violet used in the experiment were from the same batch. The transfection process, cell seeding, and culture conditions were strictly operated according to the standardized procedures to ensure consistent treatment conditions for each sample.

Scratch assay

SiHa cells were cultured in 6-well plates. When the cells grew to approximately 80% confluence, the cell monolayer was scratched with the tip of a 10-μL plastic pipette. Subsequently, the cells were washed with PBS to remove debris. The wound—healing distance was measured at 0, 12, 24, 48, and 60 h, and the cell migration amount was quantified using Image J software. To control for batch effects, the same batch of 6-well plates, cells, PBS, and plastic pipette tips was used throughout the scratch assay. During the cell-culture process, the culture conditions were kept consistent, and efforts were made to maintain the same force and angle when scratching the cells to minimize experimental errors.

Reverse transcription quantitative real-time polymerase chain reaction (RT-qPCR)

The RT-qPCR method was adopted. SiHa cells in the logarithmic growth phase were taken and divided into a control group (intervened with normal saline) and an experimental group (intervened with 600 μg/mL aqueous extract of gynostemma pentaphyllum). The cell density was adjusted to 1×10^5 cells/mL, and the cells were seeded into 6-well plates. After 24-h incubation, cells from each group were collected. The cells in each group were rinsed with PBS, and then fully lysed with TRIzol lysis buffer to extract RNA, which was then reverse-transcribed into cDNA. Specific primers (sequences shown in Table 1) were used for polymerase chain reaction (PCR) amplification after reverse-transcription of each target gene. The reaction program was as follows: 95 °C for 2 min; followed by 45 cycles of 95 °C for 10 s, 60 °C for 34 s, and 72 °C for 30 s. GAPDH was used as the internal reference gene, and the relative messenger ribonucleic acid (mRNA) expression levels of each gene were calculated using the $2^{-}\triangle\triangle CT$ method. The comparison of gene expression between the two groups was performed using a t-test, with $P<0.05$ considered statistically significant. To reduce batch effects, all reagents used in the experiment, including PBS, TRIzol lysis buffer, primers, reverse-transcription and PCR-related reagents, etc., were from the same batch. The processes of cell seeding, cell culture, RNA extraction, reverse-transcription, and PCR amplification were all carried out under the same experimental conditions by the same experimenter following standardized operating procedures.

Table 1 Gene primers sequence

Gene	Upstream primers	Downstream primers
IL6	GTGAGAGAGTGAGCGAGACA	TGTGGTTCCATCGTAGGTAG
IL1β	ATTGTGGCTGTGGAGAAG	AAGATGAAGGAAAAGAAGGTG
TNF	CACCACCATCAAGGACTCAAAT	TCAGGGAAGAATCTGGAAAGGT
TP53	GGTGCAGGGGCCACGG	TTGATGCTGTCCCCGGACGAT
PTGS2	GATGTGTATCCTCAGAGCTTTG	CGATGACAGAGATATCCCAG
Reference genes	GCCTTCCAACCATTCCCTTA	TCACGGATTTCTGTTGTGTTTC

IL6 Interleukin-6, *IL1β* Interleukin-1β, *TNF* Tumor Necrosis Factor, *TP 53* Tumorprotein P53, *PTGS2* Prostaglandin G/H Synthase 2

Results

Search for the effective components of *Gynostemmae Pentaphylli Herba* based on TCMSP

We obtained 202 ingredients by searching the TCMSP database with the keyword "*Gynostemmae Pentaphylli Herba* ". We further screened these 202 ingredients and obtained 24 active ingredients (Table 2).

Intersection targets of *Gynostemmae Pentaphylli Herba* and CIN

We obtained 85 effective compound action targets of Gynostemmae Pentaphylli Herba and 2512 CIN-related action targets. We made a Venn diagram (Fig. 1A) to obtain 52 intersection targets. The PPI network relationship diagram of the intersection target was drawn (Fig. 1B). There were 52 nodes with 217 edges, the average node degree value was 8.35, the average aggregation coefficient was 0.613, and $P < 1.0 \times 10^{-16}$. The higher degree value reflects an important role in the interaction between the active ingredient and the disease target. The top five targets in terms of degree value were Interleukin-6 (IL6), Interleukin-1β (IL1β), Tumor Necrosis Factor (TNF), Tumorprotein P53 (TP53), and Prostaglandin G/H Synthase 2 (PTGS2), respectively (Table 3).

The PPI network of the active ingredient of *Gynostemmae Pentaphylli Herba* and CIN intersection target

We constructed the target relationship diagram of the active ingredient of *Gynostemmae Pentaphylli Herba* (Fig. 2A) and the intersection target network of the active ingredient of *Gynostemmae Pentaphylli Herba* and CIN (Fig. 2B), which included 68 nodes and 180 edges. The main active ingredient MOL000098 (Quercetin) corresponds to the most targets (40), followed by MOL000351 (Rhamnazin) (17), suggesting that the above active ingredients may play a key role.

Enrichment analysis

We utilized the DAVID database to perform GO and KEGG pathway enrichment analyses on the target genes. The enrichment results were filtered based on the *P*-values corrected by the FDR. The GO analysis showed that BP was mainly enriched in positive regulation of transcription from RNA polymerase II promoter,

Table 2 Effective components of *Gynostemmae Pentaphylli Herba*

MOL ID	Effective components	OB (%)	DL
MOL000338	3'-methyleriodictyol	51.61	0.27
MOL000351	Rhamnazin	47.14	0.34
MOL000359	sitosterol	36.91	0.75
MOL004350	Ruvoside_qt	36.12	0.76
MOL004355	Spinasterol	42.98	0.76
MOL005438	Campesterol	37.58	0.71
MOL005440	Isofucosterol	43.78	0.76
MOL007475	ginsenoside f2	36.43	0.25
MOL000953	CLR	37.87	0.68
MOL000098	Quercetin	46.43	0.28
MOL009855	(24S)-Ethylcholesta-5,22,25-trans-3beta-ol	46.91	0.76
MOL009867	4α,14α-dimethyl-5α-ergosta-7,9(11),24(28)-trien-3β-ol	46.29	0.76
MOL009877	cucurbita-5,24-dienol	44.02	0.74
MOL009878	Cyclobuxine	84.48	0.70
MOL009888	Gypenoside XXXVI_qt	37.85	0.78
MOL009928	Gypenoside LXXIV	34.21	0.24
MOL009929	Gypenoside LXXIX	37.75	0.25
MOL009938	Gypenoside XII	36.43	0.25
MOL009943	Gypenoside XL	30.89	0.21
MOL009969	Gypenoside XXXV_qt	37.73	0.78
MOL009971	Gypenoside XXVII_qt	30.21	0.74
MOL009973	Gypenoside XXVIII_qt	32.08	0.74
MOL009976	Gypenoside XXXII	34.24	0.25
MOL009986	Gypentonoside A_qt	36.13	0.80

CLR is a molecular name with no full English name

OB oral bioavailability, *DL* drug likeness

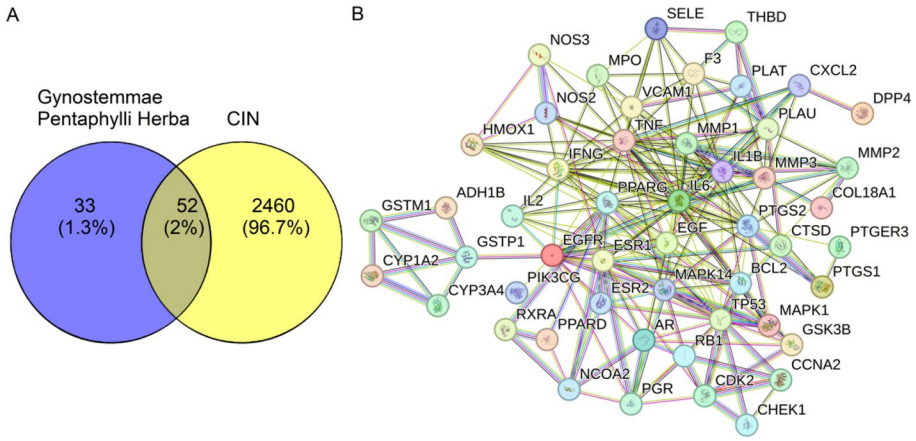

Fig. 1 Intersection targets and protein–protein interaction (PPI) network. **A** Venn diagram of *Gynostemmae Pentaphylli Herba* and cervical prelesions. The intersection of the action targets of the effective compounds of Gynostemma pentaphyllum (85 targets) and the action targets related to cervical intraepithelial neoplasia (CIN) (2,512 targets) is 52 targets. **B** Protein–protein interaction (PPI) network diagram of the intersection target of *Gynostemmae Pentaphylli Herba* and cervical intraepithelial neoplasia (CIN). IL6: Interleukin-6; IL1B: Interleukin-1 beta (IL1β); TNF: Tumor Necrosis Factor; TP53: Tumor Protein P53; PTGS2: Prostaglandin-endoperoxide synthase 2; EGFR: Epidermal Growth Factor Receptor; IFNG: Interferon-gamma; BCL2: B-cell lymphoma 2; ESR1: Estrogen Receptor 1; EGF: Epidermal Growth Factor; MAPK14: Mitogen-Activated Protein Kinase 14; PPARG: Peroxisome Proliferator-Activated Receptor-gamma; MAPK1: Mitogen-Activated Protein Kinase 1; PLAU: Plasminogen Activator, Urokinase; MMP1: Matrix Metallopeptidase 1; F3: Coagulation Factor III; VCAM1: Vascular Cell Adhesion Molecule 1; PGR: Progesterone Receptor; IL2: Interleukin-2; MMP3: Matrix Metallopeptidase 3; HMOX1: Heme Oxygenase 1; AR: Androgen Receptor; CDK2: Cyclin-Dependent Kinase 2; MMP2: Matrix Metallopeptidase 2; NOS2: Nitric Oxide Synthase 2; SELE: Selectin E; PLAT: Plasminogen Activator, Tissue-Type; NCOA2: Nuclear Receptor Co-Activator 2; MPO: Myeloperoxidase; ESR2: Estrogen Receptor 2; RB1: Retinoblastoma 1; CXCL2: C-X-C Motif Chemokine Ligand 2; GSK3B: Glycogen Synthase Kinase 3 beta; NOS3: Nitric Oxide Synthase 3; CCNA2: Cyclin A2; GSTP1: Glutathione S-Transferase P1; PTGS1: Prostaglandin-endoperoxide synthase 1; THBD: Thrombomodulin; GSTM1: Glutathione S-Transferase M1; RXRA: Retinoid X-Receptor alpha; PPARD: Peroxisome Proliferator-Activated Receptor-delta; CYP3A4: Cytochrome P450 Family 3 Subfamily A Member 4; CYP1A2: Cytochrome P450 Family 1 Subfamily A Member 2; CHEK1: Checkpoint Kinase 1; CTSD: Cathepsin D; PTGER3: Prostaglandin E Receptor 3; ADH1B: Alcohol Dehydrogenase 1B; COL18A1: Collagen Type XVIII Alpha 1 Chain; PIK3CG: Phosphatidylinositol-4,5-bisphosphate 3-kinase catalytic subunit gamma; DPP4: Dipeptidyl Peptidase 4; SELE: Selectin E

Table 3 Key targets of *Gynostemmae Pentaphylli Herba* in the treatment of CIN (top 10 by degree)

Serial number	Node name	MCC	Degree
1	IL6	55,240	27
2	IL1β	54,174	24
3	TNF	54,072	23
4	TP53	53,360	21
5	PTGS2	42,968	18
6	EGFR	52,370	18
7	IFNG	51,264	16
8	BCL2	47,180	16
9	ESR1	1346	16
10	EGF	5574	14

The screening criteria were an oral bioavailability (OB) of over 30% and a drug likeness (DL) of over 0.18. Genes were ranked according to the Maximal clique centrality (MCC) score and Degree. cervical intraepithelial neoplasia

CIN cervical intraepithelial neoplasia, *IL6* Interleukin-6, *IL1β* Interleukin-1β, *TNF* Tumor Necrosis Factor, *TP 53* Tumorprotein P53, *PTGS2* Prostaglandin G/H Synthase 2, *EGFR* epidermal growth factor receptor, *IFNG* interferon-gamma, *BCL2* B-cell lymphoma 2, *ESR1* estrogen receptor 1, *EGF* epidermal growth factor

positive regulation of gene expression, positive regulation of transcription, DNA-templated, positive regulation of cell proliferation, inflammatory response, and other biological processes; MF was mainly enriched in the cytoplasm, extracellular space, nucleoplasm, extracellular region, chromatin, and other cell functions. CC was mainly enriched in enzyme binding, zinc ion binding, heme binding, serine-type endopeptidase activity, sequence-specific DNA binding, and other cell components (Fig. 3A).

The enrichment analysis of the KEGG pathway obtained 114 signaling pathways. It is mainly enriched in Pathways in cancer, Fluid shear stress and atherosclerosis, Lipid and atherosclerosis, Chemical carcinogenesis-receptor activation, Prostate cancer, AGE-RAGE signaling pathway in diabetic complications, PI3K-Akt signaling pathway, Human cytomegalovirus infection, etc. (Fig. 3B).

Molecular docking

Protein molecules (the top 5 Degree IL6, IL1β, TNF, TP53, PTGS2) were combined with ligand small molecules (MOL000098 Quercetin, MOL000351 Rhamnazin,

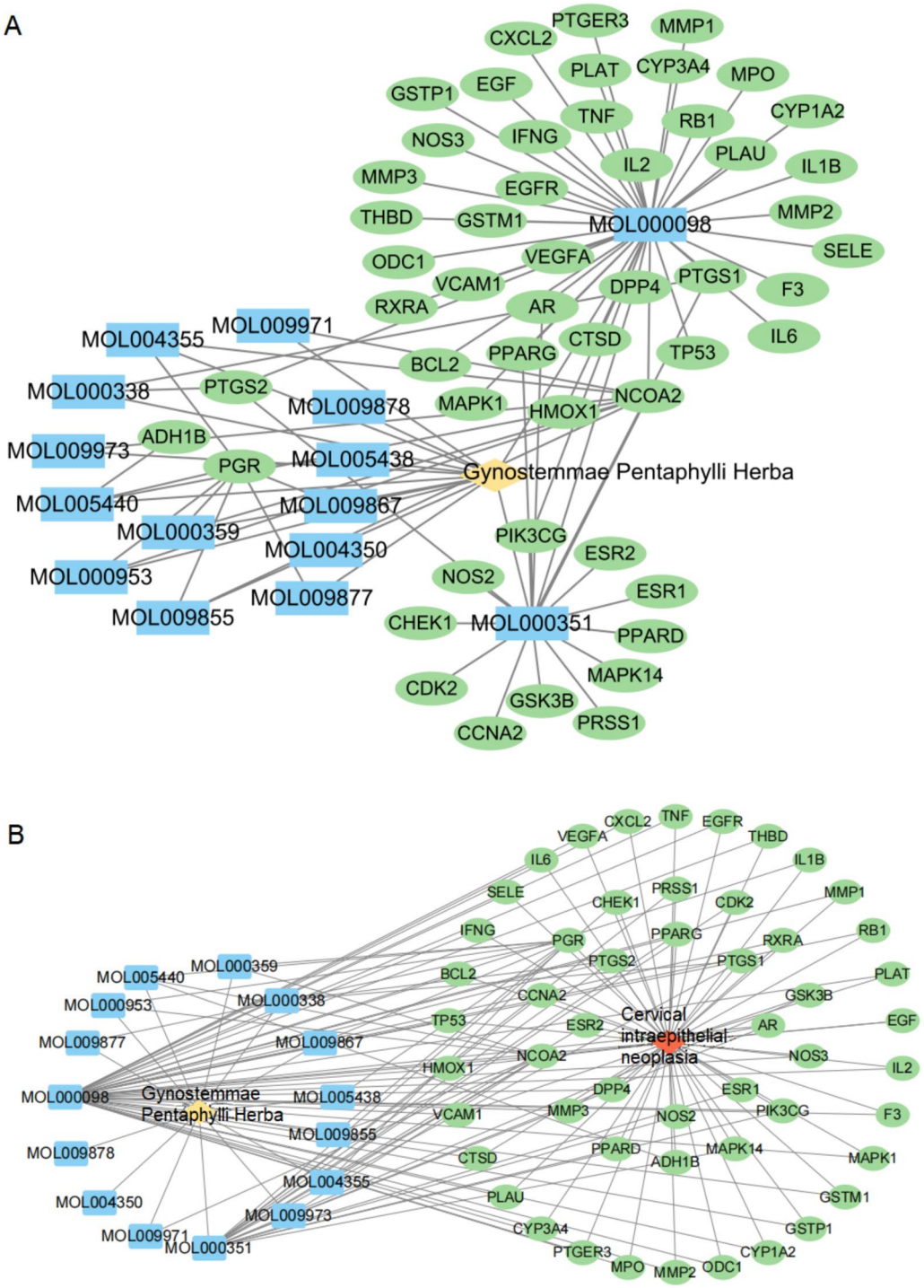

Fig. 2 Network-relationship diagrams. **A** Target-relationship diagram of the active components of gynostemma pentaphyllum. Blue labels represent active components, green labels represent targets, and yellow labels represent gynostemma pentaphyllum. **B** Network-relationship diagram of the effective active components-disease-targets of gynostemma pentaphyllum (containing 68 nodes and 180 edges). Blue labels represent active components, green labels represent targets, yellow labels represent gynostemma pentaphyllum, and red labels represent cervical intraepithelial neoplasia (CIN)

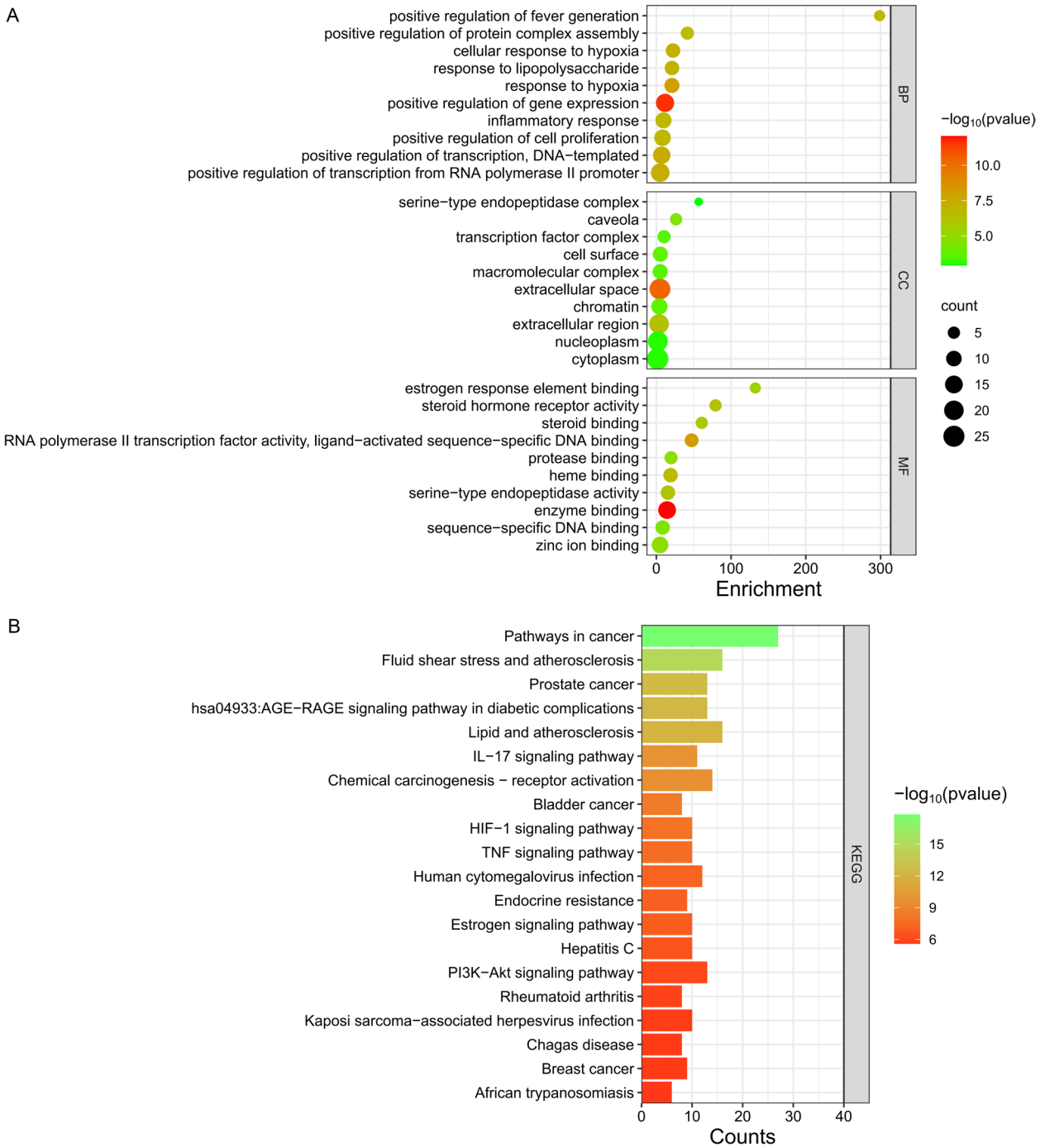

Fig. 3 Functional enrichment analysis. **A** Gene Ontology (GO) analysis diagram of key targets. **B** Kyoto Encyclopedia of Genes and Genomes (KEGG) enrichment analysis diagram of key targets. The Over-Representation (ORA) and BH methods were set for FDR correction. With the corrected false discovery rate (FDR) < 0.05 as the screening criterion, Gene Ontology (GO) [(Biological Process (BP), Molecular Function (MF), and Cellular Component (CC))] and KEGG enrichment analyses were performed. DNA: Deoxyribonucleic Acid; RNA: Ribonucleic Acid; IL-17: Interleukin-17; HIF-1: Hypoxia-Inducible Factor-1; TNF: Tumor Necrosis Factor; PI3K: Phosphatidylinositol 3-Kinase; AGE-RAGE: Advanced Glycation End-products and their Receptor

Table 4 Molecular docking binding energy

Protein	Quercetin	Rhamnazin	Gypenoside XXVII_qt	Gypenoside XXVIII_qt
IL6	−6.39	−6.66	−7.93	−8.96
IL1β	−7.01	−7.03	−8.54	−7.71
TNF	−5.61	−5.71	−6.60	−6.79
TP53	−5.73	−6.65	−7.41	−7.93
PTGS2	−8.09	−8.15	−8.38	−8.55

IL6 Interleukin-6, *IL1β* Interleukin-1β, *TNF* Tumor Necrosis Factor, *TP 53* Tumorprotein P53, *PTGS2* Prostaglandin G/H Synthase 2

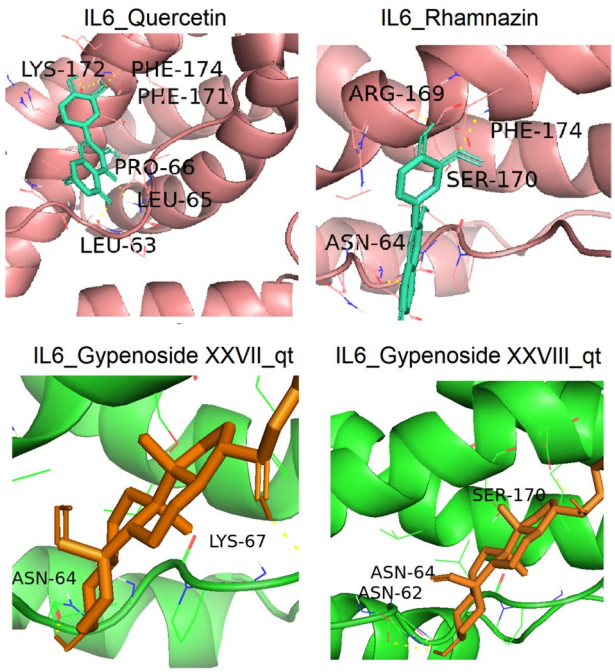

Fig. 4 The docking modes of Interleukin-6 (IL6) with Quercetin, Rhamnazin, Gypenoside XXVII_qt, and Gypenoside XXVIII_qt. The yellow dashed lines represent the hydrogen-bonding interactions in the docking

MOL009971 Gypenoside XXVII_qt, MOL009973 Gypenoside XXVIII_qt) for molecular docking. The binding energies of IL6, IL1β, TNF, TP53, and PTGS2 with Quercetin, Rhamnazin, Gypenoside XXVII_qt, and Gypenoside XXVIII_qt were all less than −5 kcal·mol^{-1}, respectively (Table 4, Figs. 4, 5, 6, 7 and 8).

Cell molecular biology experiment

Effect of Gynostemmae Pentaphylli Herba extract on CIN cell proliferation

When the concentration of *Gynostemmae Pentaphylli Herba* extract was 600 μg/mL, the OD450 value of cervical SiHa/HeLa cells was the lowest. This indicated that the survival number of HeLa/SiHa cells was the lowest under this concentration treatment, suggesting that 600 μg/mL was optimal concentration of *Gynostemmae Pentaphylli Herba* extract to inhibit HeLa/SiHa cells (Fig. 9A). After the intervention of CIN cells with 600 μg/mL *Gynostemmae Pentaphylli Herba* extract, the OD450 of HeLa/SiHa cells was significantly reduced compared with the untreated cells, which verified the strong inhibitory effect of the 600 μg/mL *Gynostemmae Pentaphylli Herba* extract extract on HeLa/SiHa cell proliferation (Fig. 9B). Plate cloning of cervical cancer SiHa/HeLa cells treated with 600 μg/mL showed that HeLa/SiHa cell proliferation decreased after treatment with *Gynostemmae Pentaphylli Herba* (Fig. 9C). Edu proliferation test and scratch test of HeLa/SiHa cells treated with 600 μg/mL showed that *Gynostemmae Pentaphylli Herba* could significantly inhibit the proliferation of cells (Fig. 9D). Scratch experiments showed that the extract of *Gynostemmae Pentaphylli Herba* could significantly inhibit SiHa cell migration (Fig. 9E).

Expression of IL6, IL1β, TNF, TP53 and PTGS2 mRNA in SiHa cells

The mRNA expressions of IL6, IL1β, TNF, and PTGS2 in the experimental group were higher compared with the control group ($t=105.700$, 32.450, 18.190, and 100.400, all $P<0.001$), and the mRNA expression of TP53 were lower than those in the control group ($t=8.362$, $P=0.001$) (Fig. 10).

Discussion

In Western medicine, CIN refers to the dysplasia of cervical epithelial cells, and its lesions mainly occur in the transformation area of the cervix, that is, the junction of squamocolumnar epithelial cells. According to its pathological changes, it can be divided into CIN I (mild atypia), CIN II (moderate atypia), and CIN III (severe atypia) [13]. According to the epidemiological survey, the incidence of CIN is related to factors such as HPV infection, autoimmune depression, early sexual life history, multiple sexual partners, and smoking. Among them, high-risk HPV infection is closely related to the disease. It is considered the primary factor in the incidence of CIN [14]. The reversal of CIN by traditional Chinese medicine

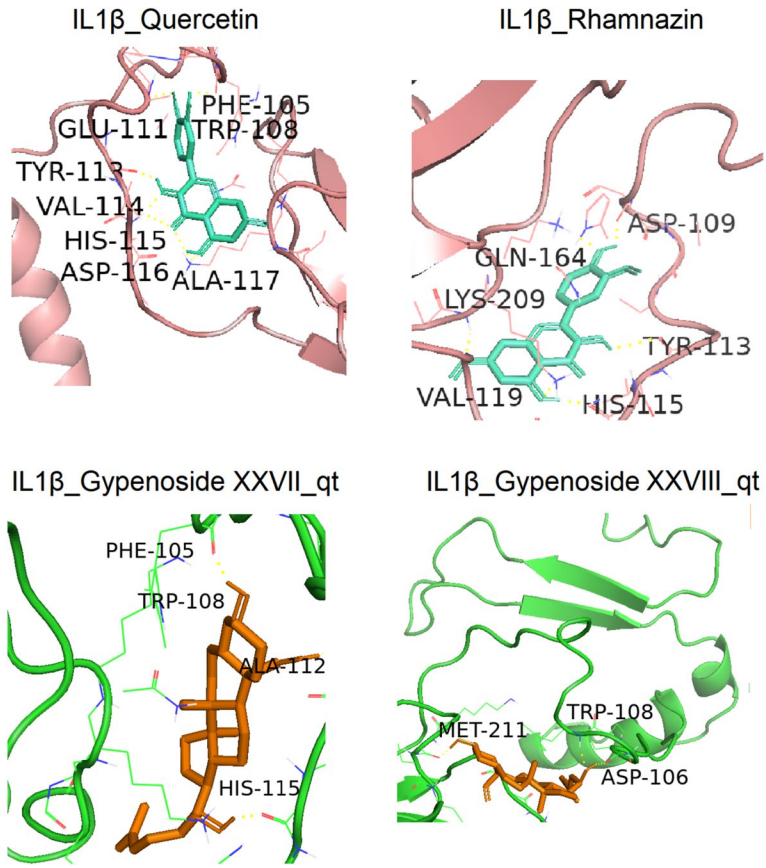

Fig. 5 The docking modes of Interleukin-1β (IL1β) with Quercetin, Rhamnazin, Gypenoside XXVII_qt, and Gypenoside XXVIII_qt. The yellow dashed lines represent the hydrogen-bonding interactions in the docking

has been confirmed in recent years [15]. Among them, *Gynostemmae Pentaphylli Herba* also plays a certain role in the CIN process, but the mechanism is unknown. Therefore, we explored the mechanism of this effect.

We collected the active ingredients of gynostemma pentaphyllum and their corresponding targets, as well as the disease targets of CIN from relevant databases. There were 52 common targets between the drug and the disease. Among these 52 intersection targets, we focused on the top five targets ranked by degree value, namely IL6, IL1β, TNF, TP53, and PTGS2. The focus on these five targets is mainly based on the following reasons. First, in numerous previous studies on CIN and related cancers, these five targets have been widely reported to be closely associated with the occurrence, development, and prognosis of CIN. For example, IL6 is closely related to the immunoregulation of the tumor microenvironment and can promote the proliferation and survival of tumor cells. IL1β can activate inflammation-related signaling pathways, influencing the progression of CIN. TNF is involved in various biological processes such as apoptosis, proliferation, and inflammatory responses, playing a significant role in the development of CIN. As an important tumor-suppressor gene, mutations or abnormal functions of TP53 frequently occur in the development of CIN and cervical cancer. PTGS2 is involved in prostaglandin synthesis, affecting the inflammatory response and proliferation of cells, and is closely related to the progression of CIN. Cervical cancer is the result of persistent HPV infection. The progression of malignant tumours is related to the inflammatory microenvironment, which is composed of T helper cells-17 (Th17) cells, a T cell subpopulation with tumorigenic properties [16]. IL6 synthesized by cervical cancer cells induces the paracrine of CCL20 in fibroblasts at the levels of promoter, mRNA, and protein. IL6 also supports the infiltration of Th17 cells, thereby shaping the local microenvironment [17]. Matamoros et al. [18] showed that women with low IL-1β expression had a 2.5 times increased risk of CIN developing into cancer. The researchers noted that monitoring the evolution of CIN through IL-1β could avoid over— or under-treatment. Studies by Long et al. [19] showed that pro-inflammatory factors IL-1β and TNF-α expression in cervical mucosa increased with the progression of

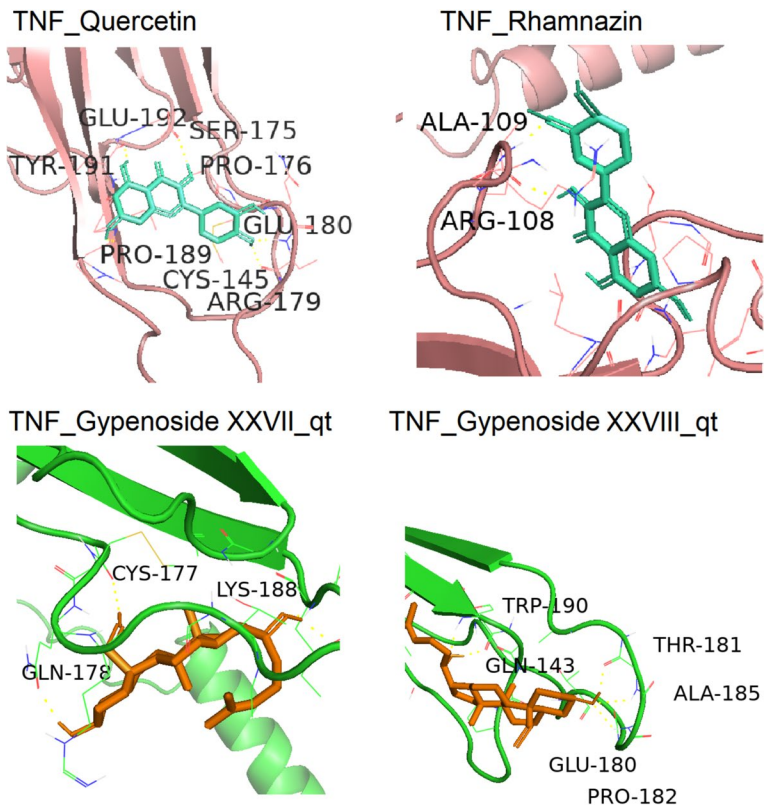

Fig. 6 The docking modes of Tumor Necrosis Factor (TNF) with Quercetin, Rhamnazin, Gypenoside XXVII_qt, and Gypenoside XXVIII_qt. The yellow dashed lines represent the hydrogen-bonding interactions in the docking

CIN, and IL-1β may be conducive to sustained HR-HPV infection. Tornesello et al. [20] found that mutations of the TP53 gene were common in CIN (grade 3). In addition, genetic variants of TP53 may influence the development of HPV and cervical cancer [21, 22]. The model of gene prediction of early cervical cancer risk shows that apposition-related genes can accurately predict early cervical cancer prognosis, and PTGS2 may play a role by influencing the polarization and mutation effect of macrophages [23]. In addition, we predicted that the main molecular targets of CIN reversal by Gypenoside were Quercetin, Rhamnazin, Gypenoside XXVII_qt, Gypenoside XXVIII_qt. Chu et al. [24] have shown that quercetin is a potential Chinese medicine component for combating cervical cancer, and its mechanism of action may be through interaction with primary protease. In addition, Ali et al. [25] showed that immunofluorescence staining showed that quercetin treatment reduced the immunoreactivity of OGT and SREBP-1 in HeLa cells, which proved that quercetin played a role in the fight against cervical cancer by reducing the o-glen acylation of AMPK. The antitumor effect of Rhamnazin was recognized in a cell experiment. Experimental results in LLC (Lewis lung carcinoma) cells of Wang et al. [26] showed that Rhamnazin enhances the anti-tumor effect of anti-PD-L1 in lung cancer mice by inhibiting the expression of programmed cell death 1 (PD-L1). Li et al. [27] showed that the mechanism of bladder cancer cell apoptosis induced by Gypenoside was closely related to the PI3K/AKT/mTOR signaling pathway. In addition, Wu et al. [28] demonstrated that gypenosides induced apoptosis of gastric cancer cells by inhibiting the PI3K/AKT/mTOR pathway and enhanced anti-tumor immunity of T cells by inhibiting PD-L1. Xiao et al. [29] showed that stranded saponins blocked cholesterol biosynthesis by inhibiting MVA pathway enzyme HMGCS1, thus inhibiting liver cancer cells. These findings reveal the exact potential of Gypenoside in the fight against cancer and, to some extent, support the idea in this study that Gypenoside may be an effective active small molecule for reversing CIN.

We further used GO and KEGG enrichment to analyze the main pathways involved in the key targets, finding that the reversal of CIN by *Gynostemmae Pentaphylli Herba* involved multiple targets, components, and pathways. The mechanism of CIN reversal by *Gynostemmae Pentaphylli Herba* may involve positive regulation of transcription from RNA polymerase II promoter, positive

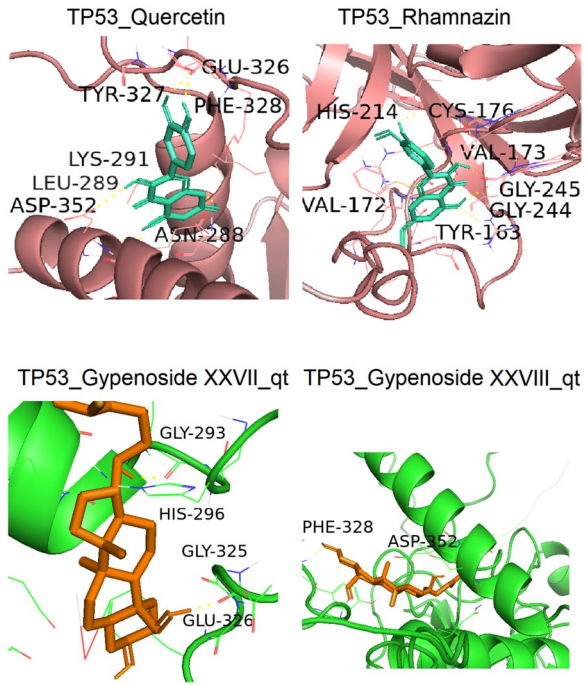

Fig. 7 The docking modes of Tumorprotein P53 (TP53) with Quercetin, Rhamnazin, Gypenoside XXVII_qt, and Gypenoside XXVIII_qt. The yellow dashed lines represent the hydrogen-bonding interactions in the docking

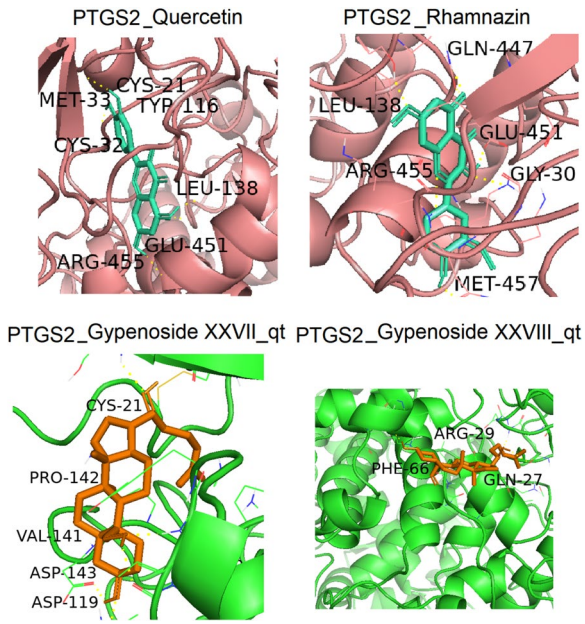

Fig. 8 The docking modes of Prostaglandin G/H Synthase 2 (PTGS2) with Quercetin, Rhamnazin, Gypenoside XXVII_qt, and Gypenoside XXVIII_qt. The yellow dashed lines represent the hydrogen-bonding interactions in the docking

regulation of gene expression, positive regulation of cell proliferation, inflammatory response and other biological processes, cytoplasm, extracellular space, nucleoplasm and other cell functions, enzyme binding, zinc ion binding, heme binding and other cell components. It mediates Pathways in cancer, Fluid shear stress and atherosclerosis, Lipid and atherosclerosis, etc. In the validation results, we used the molecular docking binding energy to evaluate the reliability of the prediction and found that protein molecules such as IL6, IL1β, TNF, TP53, PTGS2, and other active component small molecules such as Quercetin, Rhamnazin, Gypenoside XXVII_qt, Gypenoside XXVIII_qt, respectively. The key roles of IL6, IL1B, TNF, TP53, and PTGS2 genes in the reversal of CIN were verified, among which Quercetin, Rhamnazin, and Gypenoside may be the active components of gypenoside.

Cell molecular biology experiments showed that after determining the optimal concentration of *Gynostemmae Pentaphylli Herba* extract (600 μg/mL), SiHa cells were interfered with with this concentration. We found that the mRNA expressions of IL6, IL1β, TNF, and PTGS2 increased, and TP53 mRNA expression decreased in SiHa cells after the intervention of *Gynostemmae Pentaphylli Herba*, indicating that *Gynostemmae Pentaphylli Herba* can promote the expression of IL6, IL1β, TNF and PTGS2 genes in SiHa cells. It can inhibit the expression of the TP53 gene.

Our results verified that *Gynostemmae Pentaphylli Herba* exerts inhibitory effects on CIN through key targets such as IL6, IL1β, TNF, TP53, PTGS2, and related pathways. Misson et al. [30] reported that the mean serum IL-12 concentration in patients with grade II-III cervical intraepithelial neoplasia well treated with IFN-α2b was higher than in patients who failed treatment. Vahedpour et al. [31] corrected for confounding size effects of age and marital duration and determined that elevated cervical IL6 was associated with CIN. Chen et al. [32] showed that Maslinic acid showed a strong anti-IL6 effect in the CIN mouse model, which could alleviate the disease-related abnormalities of cervical tissue cell proliferation potential and apoptosis. The finding of Chen et al. is inconsistent with the results of this study, so more research data are needed to confirm the effect of *Gynostemmae Pentaphylli Herba* on IL6 expression in CIN. However, we cannot determine why *Gynostemmae Pentaphylli Herba* promoted or inhibited the above gene expression in SiHa cells, and further experimental investigation is needed.

There are limitations to this study. Although we were able to predict the mechanism of CIN reversal by *Gynostemmae Pentaphylli Herba* using network pharmacology and data mining methods, we only theoretically analyzed possible active ingredients, targets, and

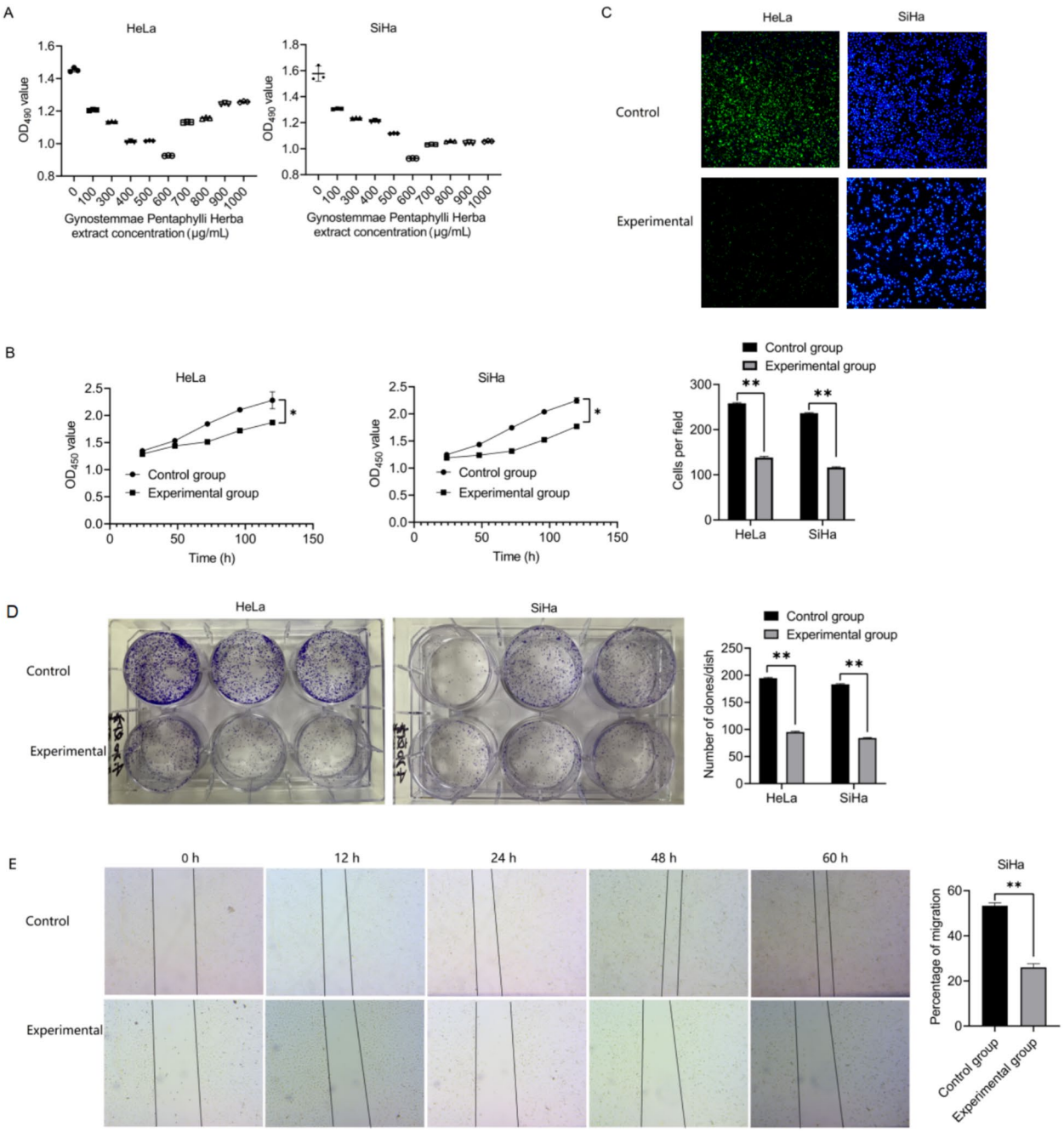

Fig. 9 Cell molecular biology experiment. **A** The effect of *Gynostemmae Pentaphylli Herba* extract on the proliferation rate of HeLa/SiHa cells; **B** The CCK8 growth curve of HeLa/SiHa cells treated with 600 μg/mL; **C** Plate cloning of HeLa/SiHa cells treated with 600 μg/mL; **D** EdU proliferation experiment of HeLa/SiHa cells treated with 600 μg/mL; (E) Scratch test of SiHa cells treated with 600 μg/mL. OD: optical density

pathways but could not fully determine the specific mechanism of drug active ingredients on CIN, so it is necessary to carry out basic experiments for verification. In addition, this study obtained data from a large database or software simulation. It is impossible to accurately judge the intensity of intermolecular interaction and difficult to exclude the influence of factors such as the origin and quality of *Gynostemmae Pentaphylli Herba* on the results. Therefore, future research needs to focus on solving these problems and verify the research conclusions.

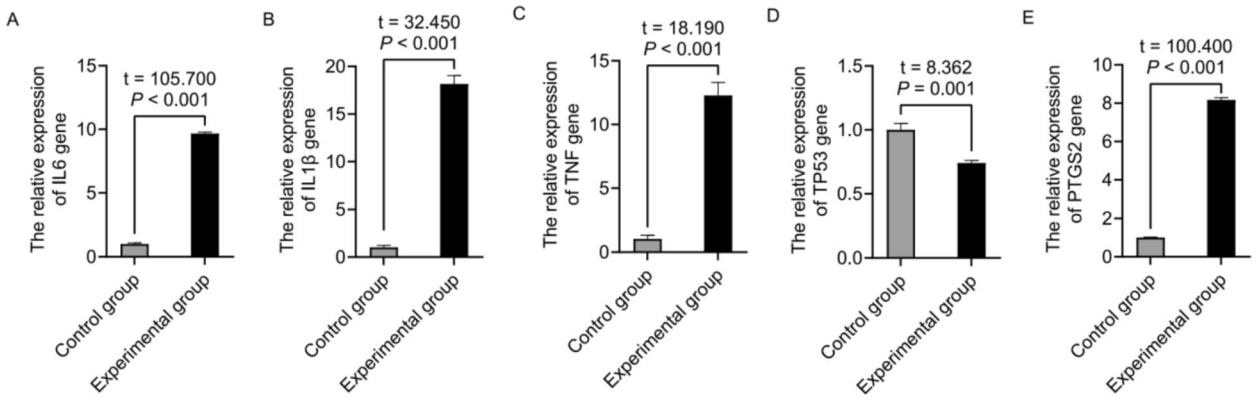

Fig. 10 Messenger ribonucleic acid (mRNA) expression of Interleukin-6 (IL6), Interleukin-1β (IL1β), Tumor Necrosis Factor (TNF), Tumorprotein P53 (TP53), and Prostaglandin G/H Synthase 2 (PTGS2) in SiHa cells. The mRNA expressions of IL6, IL1β, TNF, and PTGS2 in the experimental group were higher than those in the control group, and the mRNA expressions of TP53 were lower than those in the control group ($P < 0.05$)

In summary, *Gynostemmae Pentaphylli Herba* may reverse CIN through targeted action of Quercetin, Rhamnazin, and gypenosides, as well as various pathways. Our study preliminarily explored the pharmacodynamic components and mechanism of the reversal of CIN by *Gynostemmae Pentaphylli Herba* and verified the possible mechanism of action by cell and molecular biology experiments to understand the pharmacological mechanism of *Gynostemmae Pentaphylli Herba* in CIN and provide data reference for the research and development of new drugs and clinical trials, which will be of great significance for clinical treatment decisions.

Acknowledgements
We would like to thank Editage (https://www.editage.cn) for English language editing.

Author's contributions
H.W. and Y.C. have joint authorship and have contributed equally for this publication. H.W. and Y.C. designed the study. H.W. drafted the manuscript. Y.C. and T.L. performed the analysis. T.L. contributed to interpretation of the results. Y.C. reviewed and edited the manuscript. All authors contributed to the article and approved the submitted version.

Funding
This research was supported by Quanzhou City Science and Technology Program(grant number 2023N011S).

Data availability
Data could be requested from the corresponding author.

Declarations

Ethics approval and consent to participate
This study was approved by the Ethics Committee of Quanzhou Medical College.

Consent for publication
Not applicable.

Competing interests
The authors declare no competing interests.

Author details
[1]Department of Obstetrics and Gynecology, Quanzhou Medical College, Quanzhou, Fujian 362100, China. [2]Department of Ultrasound, Jinjiang Municipal Hospital, Fujian 362200, China. [3]School of Marxism, Quanzhou Medical College, Quanzhou, Fujian 362100, China.

Received: 3 November 2024 Accepted: 3 March 2025
Published online: 21 March 2025

References

1. Singh D, Vignat J, Lorenzoni V, Eslahi M, Ginsburg O, Lauby-Secretan B, Arbyn M, Basu P, Bray F, Vaccarella S. Global estimates of incidence and mortality of cervical cancer in 2020: a baseline analysis of the WHO Global Cervical Cancer Elimination Initiative. Lancet Glob Health. 2023;11(2):e197-e206. https://doi.org/10.1016/S2214-109X(22)00501-0. Epub 2022 Dec 14. PMID: 36528031; PMCID: PMC9848409.
2. Wang J, Zheng CX, Ma CL, Zheng XX, Lv XY, Lv GD, Tang J, Wu GH. Raman spectroscopic study of cervical precancerous lesions and cervical cancer. Lasers Med Sci. 2021;36(9):1855–1864. https://doi.org/10.1007/s10103-020-03218-5. Epub 2021 Jan 6. PMID: 33404885; PMCID: PMC8594213.
3. Guo F, Kong WN, Li DW, Zhao G, Wu HL, Anwar M, Shang XQ, Sun QN, Ma CL, Ma XM. Low Tumor Infiltrating Mast Cell Density Reveals Prognostic Benefit in Cervical Carcinoma. Technol Cancer Res Treat. 2022;21:15330338221106530. https://doi.org/10.1177/15330338221106530.PMID:35730194;PMCID:PMC9228650.
4. Bowden SJ, Doulgeraki T, Bouras E, Markozannes G, Athanasiou A, Grout-Smith H, Kechagias KS, Ellis LB, Zuber V, Chadeau-Hyam M, Flanagan JM, Tsilidis KK, Kalliala I, Kyrgiou M. Risk factors for human papillomavirus infection, cervical intraepithelial neoplasia and cervical cancer: an umbrella review and follow-up Mendelian randomisation studies. BMC Med. 2023;21(1):274. https://doi.org/10.1186/s12916-023-02965-w. PMID: 37501128;PMCID:PMC10375747.
5. Monti M, D'Aniello D, Scopelliti A, Tibaldi V, Santangelo G, Colagiovanni V, Giannini A, DI Donato V, Palaia I, Perniola G, Giancotti A, Muzii L, Benedetti Panici P. Relationship between cervical excisional treatment for cervical intraepithelial neoplasia and obstetrical outcome. Minerva Obstet Gynecol. 2021;73(2):233–246. https://doi.org/10.23736/S2724-606X.20.04678-X. Epub 2020 Nov 3. PMID: 33140628.
6. Gao M, Liu JJ, Wang D. The anti-proliferation effect of gypenosides on cervical cancer HeLa cells and its molecular mechanism. Tumor,2013,33(10):868–872. https://doi.org/10.3781/j.issn.1000-7431.2013.10.004.
7. Lai ZQ, Wu LN, Li YH, Tang YX.Preparation and antitumor study of aptamer modified gynostemma pentaphyllum targeted li-posomes. Journal of

Guangxi Medical University ,2022,39(3):450–455. https://doi.org/10.16190/j.cnki.45-1211/r.2022.03.018.
8. Ma C, Zhao J, Zheng G, Wu S, Wu R, Yu D, Liao J, Zhang H, Liu L, Jiang L, Qian F, Zeng H, Wu G, Lu Z, Ye J, Zhang W. Qijiao Shengbai Capsule alleviated leukopenia by interfering leukotriene pathway: Integrated network study of multi-omics. Phytomedicine. 2024;128: 155424. https://doi.org/10.1016/j.phymed.2024.155424. (Epub 2024 Feb 7 PMID: 38537441).
9. Wang ZY, Li MZ, Li WJ, Ouyang JF, Gou XJ, Huang Y. Mechanism of action of Daqinjiao decoction in treating cerebral small vessel disease explored using network pharmacology and molecular docking technology. Phytomedicine. 2023;108: 154538. https://doi.org/10.1016/j.phymed.2022.154538. (Epub 2022 Nov 9 PMID: 36370638).
10. Ji H, Li K, Xu W, Li R, Xie S, Zhu X. Prediction of the Mechanisms by Which Quercetin Enhances Cisplatin Action in Cervical Cancer: A Network Pharmacology Study and Experimental Validation. Front Oncol. 2022;11: 780387. https://doi.org/10.3389/fonc.2021.780387. PMID:35070983;PMCID:PMC8770278.
11. Yin Z, Hua X, Lu M. Integrated network pharmacology and metabolomics to dissect the mechanisms of naringin for treating cervical cancer. Comb Chem High Throughput Screen. 2023. https://doi.org/10.2174/1386207326666230504124030. Epub ahead of print. PMID: 37143280.
12. Campos-Parra AD, Pérez-Quintanilla M, Martínez-Gutierrez AD, Pérez-Montiel D, Coronel-Martínez J, Millan-Catalan O, De León DC, Pérez-Plasencia C. Molecular Differences between Squamous Cell Carcinoma and Adenocarcinoma Cervical Cancer Subtypes: Potential Prognostic Biomarkers. Curr Oncol. 2022;29(7):4689–702. https://doi.org/10.3390/curroncol29070372. PMID:35877232;PMCID:PMC93223650.
13. Liu H, Liang H, Li D, Wang M, Li Y. Association of Cervical Dysbacteriosis, HPV Oncogene Expression, and Cervical Lesion Progression. Microbiol Spectr. 2022;10(5):e0015122. https://doi.org/10.1128/spectrum.00151-22. Epub 2022 Aug 29. PMID: 36036584; PMCID: PMC9602310.
14. Kumari S, Bhor VM. Association of cervicovaginal dysbiosis mediated HPV infection with cervical intraepithelial neoplasia. Microb Pathog. 2021;152: 104780. https://doi.org/10.1016/j.micpath.2021.104780. (Epub 2021 Feb 3 PMID: 33545325).
15. Huang S, Qi Y, Chen S, He B, Chen X, Xu J. Effect of heat-clearing and dampness-eliminating Chinese medicine for high-risk cervical cancer papillomavirus infection: a systematic review and meta-analysis of randomized controlled trials. Front Med (Lausanne). 2023;10:1022030. https://doi.org/10.3389/fmed.2023.1022030. PMID:37692777;PMCID: PMC10484520.
16. Jesus ACC, Meniconi MCG, Galo LK, Duarte MIS, Sotto MN, Pagliari C. Plasmacytoid Dendritic Cells, the Expression of the Stimulator of Interferon Genes Protein (STING) and a Possible Role of Th17 Immune Response in Cervical Lesions Mediated by Human Papillomavirus. Indian J Microbiol. 2023;63(4):588–595. https://doi.org/10.1007/s12088-023-01117-1. Epub 2023 Nov 9. PMID: 38031606; PMCID: PMC10682341.
17. Walch-Rückheim B, Mavrova R, Henning M, Vicinus B, Kim YJ, Bohle RM, Juhasz-Böss I, Solomayer EF, Smola S. Stromal Fibroblasts Induce CCL20 through IL6/C/EBPβ to Support the Recruitment of Th17 Cells during Cervical Cancer Progression. Cancer Res. 2015;75(24):5248–59. https://doi.org/10.1158/0008-5472.CAN-15-0732. (Epub 2015 Dec 2 PMID: 26631268).
18. Matamoros JA, da Silva MIF, de Moura PMMF, Leitão MDCG, Coimbra EC. Reduced Expression of IL-1β and IL-18 Proinflammatory Interleukins Increases the Risk of Developing Cervical Cancer. Asian Pac J Cancer Prev. 2019;20(9):2715–2721. https://doi.org/10.31557/APJCP.2019.20.9.2715. PMID: 31554368; PMCID: PMC6976845.
19. Long DL, Song HL, Qu PP. Cytokines profiles in cervical mucosa in patients with cervical high-risk human papillomavirus infection. J Infect Dev Ctries. 2021;15(5):719–725. https://doi.org/10.3855/jidc.12147. PMID: 34106897.
20. Tornesello ML, Annunziata C, Buonaguro L, Losito S, Greggi S, Buonaguro FM. TP53 and PIK3CA gene mutations in adenocarcinoma, squamous cell carcinoma and high-grade intraepithelial neoplasia of the cervix. J Transl Med. 2014;12:255. https://doi.org/10.1186/s12967-014-0255-5. PMID:25220666;PMCID:PMC4174264.
21. Koshiol J, Hildesheim A, Gonzalez P, Bratti MC, Porras C, Schiffman M, Herrero R, Rodriguez AC, Wacholder S, Yeager M, Chanock SJ, Burk RD, Wang SS. Common genetic variation in TP53 and risk of human papillomavirus persistence and progression to CIN3/cancer revisited. Cancer Epidemiol Biomarkers Prev. 2009;18(5):1631–7. https://doi.org/10.1158/1055-9965.EPI-08-0830. PMID:19423538;PMCID:PMC2764239.
22. Parra-Herran C, Nucci MR, Singh N, Rakislova N, Howitt BE, Hoang L, Gilks CB, Bosse T, Watkins JC. HPV-independent, p53-wild-type vulvar intraepithelial neoplasia: a review of nomenclature and the journey to characterize verruciform and acanthotic precursor lesions of the vulva. Mod Pathol. 2022;35(10):1317–26. https://doi.org/10.1038/s41379-022-01079-7. (Epub 2022 Apr 18 PMID: 35437330).
23. Zou C, Xu F, Shen J, Xu S. Identification of a Ferroptosis-Related Prognostic Gene PTGS2 Based on Risk Modeling and Immune Microenvironment of Early-Stage Cervical Cancer. J Oncol. 2022;2022:3997562. https://doi.org/10.1155/2022/3997562. PMID:35432535;PMCID:PMC9012634.
24. Chu M, Ji H, Li K, Liu H, Peng M, Wang Z, Zhu X. Investigating the potential mechanism of quercetin against cervical cancer. Discov Oncol. 2023;14(1):170. https://doi.org/10.1007/s12672-023-00788-y. PMID:37704909;PMCID:PMC10499770.
25. Ali A, Kim MJ, Kim MY, Lee HJ, Roh GS, Kim HJ, Cho GJ, Choi WS. Quercetin induces cell death in cervical cancer by reducing O-GlcNAcylation of adenosine monophosphate-activated protein kinase. Anat Cell Biol. 2018;51(4):274–283. https://doi.org/10.5115/acb.2018.51.4.274. Epub 2018 Dec 29. PMID: 30637162; PMCID: PMC6318463.
26. Wang SS, Liu Y, Zhang XT, Yu DQ. Rhamnazin Enhanced Anti-Tumor Efficacy of Anti-PD-1 Therapy for Lung Cancer in Mice through Inhibition of PD-L1 Expression. Tohoku J Exp Med. 2023;260(1):63–73. https://doi.org/10.1620/tjem.2023.J014. (Epub 2023 Feb 23 PMID: 36823182).
27. Li X, Liu H, Lv C, Du J, Lian F, Zhang S, Wang Z, Zeng Y. Gypenoside-Induced Apoptosis via the PI3K/AKT/mTOR Signaling Pathway in Bladder Cancer. Biomed Res Int. 2022;2022:9304552. https://doi.org/10.1155/2022/9304552. PMID:35402614;PMCID:PMC8984741.
28. Wu H, Lai W, Wang Q, Zhou Q, Zhang R, Zhao Y. Gypenoside induces apoptosis by inhibiting the PI3K/AKT/mTOR pathway and enhances T-cell antitumor immunity by inhibiting PD-L1 in gastric cancer. Front Pharmacol. 2024;15:1243353. https://doi.org/10.3389/fphar.2024.1243353. PMID: 38482051;PMCID:PMC10933075.
29. Xiao MY, Li FF, Xie P, Qi YS, Xie JB, Pei WJ, Luo HT, Guo M, Gu YL, Piao XL. Gypenosides suppress hepatocellular carcinoma cells by blocking cholesterol biosynthesis through inhibition of MVA pathway enzyme HMGCS1. Chem Biol Interact. 2023;383: 110674. https://doi.org/10.1016/j.cbi.2023.110674. (Epub 2023 Aug 19 PMID: 37604220).
30. Misson DR, Abdalla DR, Borges AM, Shimba DS, Adad SJ, Michelin MA, Murta EF. Cytokine serum levels in patients with cervical intraepithelial neoplasia grade II-III treated with intralesional interferon-α 2b. Tumori. 2011;97(5):578–84.
31. Vahedpour Z, Abedzadeh-Kalahroudi M, Sehat M, Piroozmand A, Memar M. Comparison of Cervical Levels of Interleukins-6 and -8 in Patients with and without Cervical Intraepithelial Neoplasia. Asian Pac J Cancer Prev. 2021;22(4):1225–1230. https://doi.org/10.31557/APJCP.2021.22.4.1225. PMID: 33906316; PMCID: PMC8325114.
32. Chen J, Wang L. Maslinic Acid Inhibits Cervical Intraepithelial Neoplasia by Suppressing Interleukin- 6 and Enhancing Apoptosis in a Mouse Model. Anticancer Agents Med Chem. 2022;22(3):579–85. https://doi.org/10.2174/1871520621666210903143922. (PMID: 34477530).

Publisher's Note